Direct Two-Nucleon Pickup in (d, α) Reactions*

J. R. CURRY, W. R. COKER, AND P. J. RILEY
University of Texas at Austin, Texas 78712

(Received 14 March 1969)

Angular distributions for the (d, α) reactions on ^{13}C, ^{14}N, and ^{31}P targets have been measured in the 10–12-MeV incident-deuteron energy range. The $^{31}P(d, \alpha)^{29}Si$ measurements have been repeated at a deuteron energy of 33.7 MeV. The experimental angular distributions for the first three α groups in each reaction have been fitted and analyzed using a zero-range distorted-wave Born-approximation two-particle pickup calculation. Nuclear-structure factors were computed from shell-model wave functions and tested against the experimental results. The shapes of the angular distributions and the relative magnitudes of the experimental cross sections are both found to be successfully predicted by the theory. The ground-state reactions have also been analyzed using a simple cluster-transfer approximation, and the results are compared with the more exact analysis. The cluster-transfer approximation is shown to predict correctly the dominant L, J values contributing to the (d, α) reactions, but cannot give absolute cross sections.

I. INTRODUCTION

THE use of direct single-particle transfer reactions in nuclear spectroscopy has been extensive. Until recently, however, studies involving the transfer of two or more nucleons have received relatively little investigation. This lack of attention is not primarily due to experimental difficulties, but is caused by the relatively recent appearance of formulations of direct-reaction theory capable of analyzing two-nucleon transfer reactions.[1–5]

Initial attempts to analyze two-nucleon transfer reactions were based on a plane-wave Born-approximation (PWBA) treatment.[6,7] The realization of the importance of optical distortion in the entrance and exit channels, and the subsequent success of a distorted-wave theory in one-nucleon transfer reactions, led to the hope that a distorted-wave Born approximation (DWBA) might give an adequate description of the direct two-nucleon transfer process. To alleviate some of the many difficulties which arise in a realistic description of two-nucleon transfer, the recent DWBA theories assume certain correlations between the transferred nucleons, and thus, impose stringent conditions on the possible population of nuclear levels. If such theories prove to give an adequate description of the actual process, then the use of two-nucleon transfer reactions in nuclear spectroscopy appears hopeful. Indeed, spectroscopy through the direct transfer of two nucleons should prove to be a fruitful tool, since these reactions can readily reach states that have two holes or particles excited relative to some ground state. Such states often are weakly or not at all excited in single-nucleon transfer.

The purpose of this work is to test the possibility of extracting spectroscopic information from one particular type of two-nucleon transfer reaction, namely, the (d, α) reaction. The major part of the analysis used is based on the two-nucleon transfer form-factor calculation of Bayman and Kallio.[8] In contrast to other recent theories,[2] this calculation does not depend upon the exclusive use of harmonic-oscillator wave functions for the two individual particles transferred. This allows the bound-state problem to be solved using the more realistic Woods-Saxon potential. In addition to this approach to the problem, analyses which are based on a less realistic "cluster-model" calculation have also been carried out as a test of the sensitivity of DWBA results to the details of the two-nucleon wave function. Most of the present work is based on the analysis of the $^{31}P(d, \alpha)^{29}Si$ reaction at a bombarding energy of 33.7 MeV. For comparison, the (d, α) reactions on ^{31}P, ^{13}C, and ^{14}N were also studied in the 10–12-MeV incident-deuteron energy range. Attempts were made to fit the ground and first two excited state reactions for each of the three targets, taking into account the various anticipated configurations of the target and residual nuclei.

II. EXPERIMENTAL PROCEDURES

For the higher-energy work, a 33.7-MeV deuteron beam was provided by the Oak Ridge isochronous cyclotron. After being passed through a 153° analyzing magnet, the beam was directed into the experimental area and then focused onto a target located in the center of a 30-in.-diam precision scattering chamber. Following the method of Hooten,[9] the ^{31}P targets were prepared by

* Work supported in part by the U.S. Atomic Energy Commission.

[1] C. L. Lin and S. Yoshida, Progr. Theoret. Phys. **32**, 885 (1964).
[2] N. K. Glendenning, Ann. Rev. Nucl. Sci. **13**, 191 (1963).
[3] E. M. Henley and D. U. L. Yu. Phys. Rev. **133**, B1445 (1964).
[4] B. Imaniski, Progr. Theoret. Phys. **32**, 542 (1964).
[5] J. Janecke, Nucl. Phys. **48**, 129 (1963).
[6] H. C. Newns, Proc. Phys. Soc. (London) **76**, 489 (1960).
[7] N. K. Glendenning, Nucl. Phys. **29**, 109 (1962).
[8] B. F. Bayman and A. Kallio. Phys. Rev. **156**, 1121 (1967).
[9] B. W. Hooten, Nucl. Instr. Methods **27**, 338 (1964).

successive evaporations of red phosphorus onto thin carbon backings until a target thickness of about 510 $\mu g/cm^2$ was obtained. The α particles were detected and distinguished from the other reaction products by means of a ΔE-E solid-state detector telescope and summing electronics. A computer program[10] allowed the resulting two-dimensional spectra to be reduced on line to conventional particle-energy–versus–intensity plots. Two typical α-particle spectra thus obtained are shown in Fig. 1. With this experimental arrangement, 18 α groups were observed, leading to the ground and various excited states in ^{29}Si. The first six $T=0$ states in ^{10}B, resulting from the (d, α) reactions on the ^{12}C target backing, were also easily resolved. The over-all experimental resolution was about 70 keV.

The Q values for all the observed α groups were determined from the known Q values of the first three α groups in the ^{31}P(d, α) reaction and the first three groups of the ^{12}C(d, α) reaction. Differential cross sections were measured at 13 angles between 11° and 60° in the laboratory. The resulting angular distributions for the various ^{31}P(d, α) reactions are shown in Fig. 2. The error bars are due to counting statistics. The 2.044-MeV level is preferentially populated in this (d, α) reaction by a factor of about 10 above the ground state. All of the angular distributions are characterized by strong forward peaking, which is often indicative of predominantly direct reactions.

Deuterons in the 10–12-MeV energy range were obtained from the University of Texas EN tandem Van de Graaff accelerator. From the 90° analyzing magnet, the beam was focused onto a target located in the center of an 18-in.-diam scattering chamber. Except for the

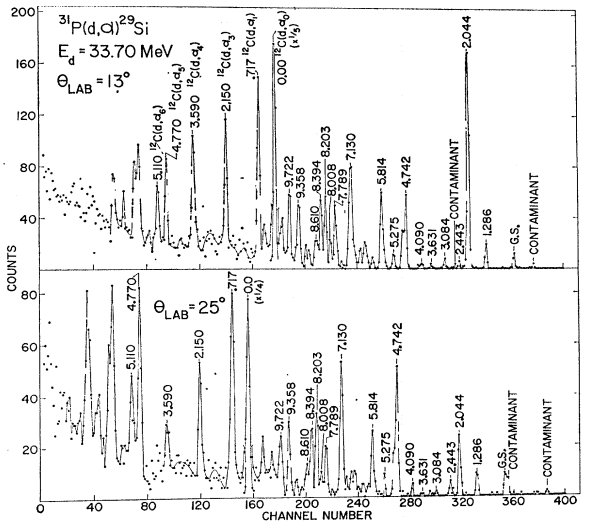

FIG. 1. Typical α-particle spectra for the ^{31}P$(d, \alpha)^{29}$Si reactions at 33.7 MeV. (G.S.≡ground state.)

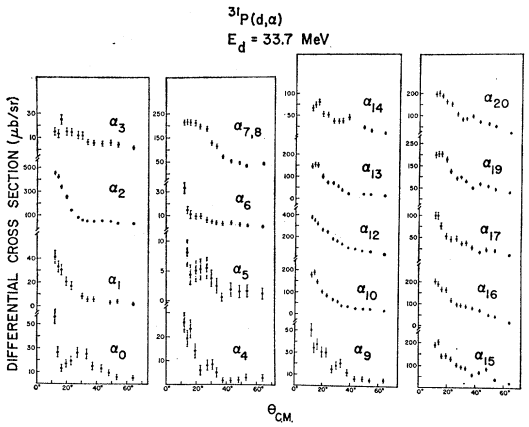

FIG. 2. Experimental angular distributions for the ^{31}P(d, α) reactions at an incident deuteron energy of 33.7 MeV.

^{13}C target, which was obtained from the University of Pennsylvania, all targets were made at the University of Texas Center for Nuclear Studies. The ^{14}N target was prepared by the evaporation of adenine ($C_5H_3N_4 \cdot NH_2$) onto thin carbon backings. The ^{31}P target was prepared in a manner identical to that described above. For this lower energy work, the thicknesses of the ^{13}C, ^{14}N, and ^{31}P targets were respectively 59, 320, and 160 $\mu g/cm^2$. The α particles were detected by means of 300-μ-depletion-depth solid-state surface-barrier detectors. The output of each detector, after suitable amplification, was routed to a Victoreen 1024-channel analog-to-digital converter (ADC). The digital information from the ADC was stored in an on-line PDP-7 computer and plotted on a line printer. Typical spectra for the (d, α) reactions on ^{14}N and ^{31}P are shown in Fig. 3. Differential cross sections were measured in 5-deg intervals from 20° to 170° in the laboratory, and are shown in Fig. 4.

In the 10–12-MeV deuteron energy range, one anticipates a noticeable contribution to the cross sections from the compound nucleus. The general backward peaking and the relative symmetry about 90° for several of these experimental angular distributions are roughly indicative that a compound-nucleus mechanism may indeed make an important contribution to the reactions. It is therefore anticipated that the theoretical fits to these data will not give as definitive a test of the theory as the work done at 33.7 MeV.

III. THEORY

The experimental angular distributions for the first three α groups in each reaction were fitted and analyzed using a zero-range DWBA two-particle pickup calculation.[8,11] This approach assumes that the (d, α) reaction proceeds by the pickup of a neutron-proton pair in a *relative* $l=0$, $S=1$, $T=0$ state from the target nucleus.

[10] E. Newman (unpublished).

[11] T. Tamura, Computer Phys. Commun. (to be published).

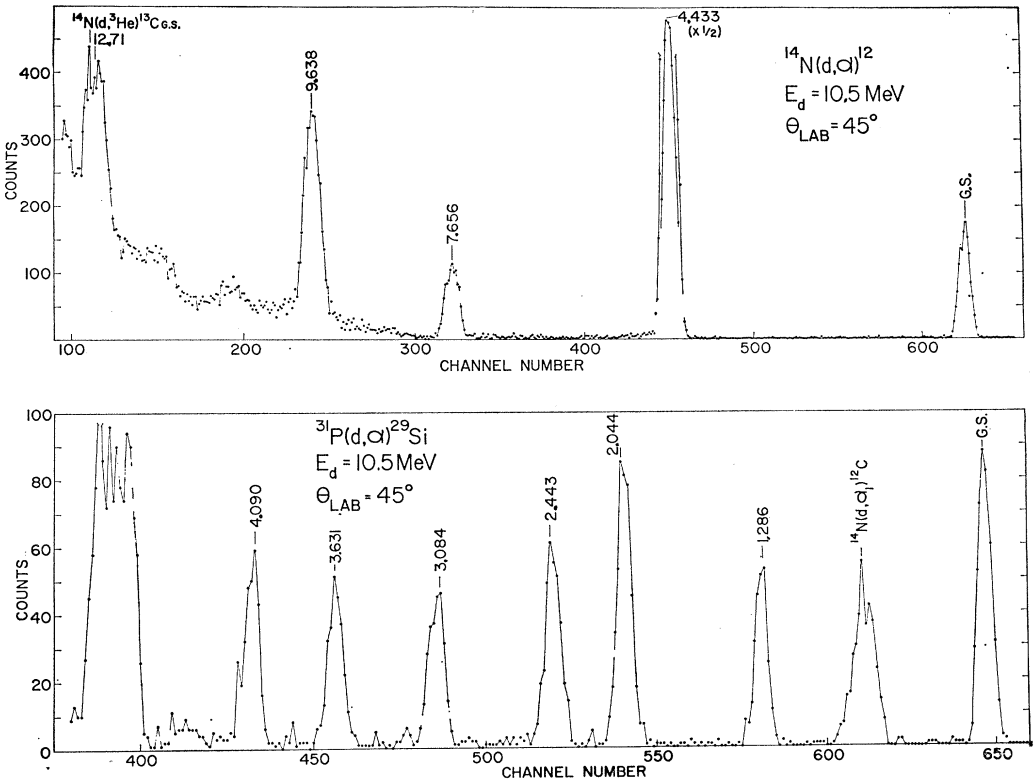

FIG. 3. Typical spectra of the ^{14}N(d, α) and ^{31}P(d, α) reactions observed at 10.5 MeV.

Therefore, the reaction will proceed predominantly from the components of the target-nucleus shell-model wave function where that relative two-particle configuration is strong, to states of the final nucleus with the same isotopic spin as the target nucleus and containing configurations with the core unexcited.

Keeping such underlying assumptions in mind, the cross section for the (d, α) reaction may be written as

$$d\sigma/d\Omega \propto \sum_{LJM_L} \Big| \sum_{\gamma} \beta_{\gamma L1J} \times \langle (l_1\tfrac{1}{2})_{j1}(l_2\tfrac{1}{2})_{j2} \,|\, (l_1l_2)_L(\tfrac{1}{2}\tfrac{1}{2})_1\rangle_J B_{\gamma L}{}^{M_L} \Big|^2, \quad (1)$$

where L and J are, respectively, the orbital and total angular momentum of the transferred n-p pair, and γ represents all other quantum numbers needed to specify the two-nucleon state of the transferred pair: $\gamma \equiv n_1l_1j_1n_2l_2j_2$. The term in brackets is the $LS \rightleftarrows jj$ transformation coefficient. The nuclear-structure information, which is contained in the factor β, will be discussed later. We first consider the kinematic factor $B_{\gamma L}{}^{M_L}$, which is the transition amplitude for transferring a neutron-proton pair in the state described by γ, L, and M_L. This transfer amplitude is explicitly written in the zero-range approximation as

$$B_{\gamma L}{}^{M_L} \propto \int \Phi_{\alpha B}{}^{(-)*}(\mathbf{k}_\alpha, \mathbf{R}) F_{L\gamma}(R) Y_L{}^{M_L}(\hat{R}) \Phi_{dA}{}^{(+)}(\mathbf{k}_d, \mathbf{R})\, d\mathbf{R}, \quad (2)$$

where $\Phi_{dA}{}^{(+)}$ and $\Phi_{\alpha B}{}^{(+)}$ are the distorted waves for the entrance and exit channels, respectively. They are generated from optical-model potentials which describe the corresponding observed elastic scattering. Calculations for the two-nucleon transfer form factors $F_{L\gamma}(R)$ were made through the use of a computer code written by Bayman.[12] The computer code recouples the angular momenta of the two single-particle wave functions and then expands the resultant function in terms of relative and c.m. coordinates. A relative s state is required for this expansion. Woods-Saxon wave functions are used for the individual particles. A Gaussian α-particle function is used in an overlap integration over the relative coordinates of the two particles to yield a function of the c.m. coordinate only. This c.m. function which appears in the above equation is explicitly represented by

$$F_{L\gamma}(R) \equiv R^{-1} \int \exp(-4\eta^2 r^2) f_{0,L}{}^{L}(r, R)\, dr, \quad (3)$$

where the distribution function $f_{0,L}{}^{L}(r, R)$ is computed from the individual-particle Woods-Saxon functions as outlined in Ref. 8. The assumed Gaussian form,

$$\phi_\alpha = [N/(4\pi)^{3/2}] \exp(-\eta^2 \textstyle\sum r_{ij}{}^2), \quad (4)$$

for the α-particle wave function allows it to be separated

[12] B. F. Bayman (private communication).

into three independent functions, which, themselves, depend separately and respectively upon the relative coordinate of the two transferred particles ($\mathbf{r}$), the relative coordinate of the neutron and proton in the incident deuteron ($\mathbf{r}_d$), and the relative coordinate between the c.m. of the incident deuteron and the c.m. of the two transferred nucleons ($\boldsymbol{\varrho}$). The rearrangement potential V which is also a function of $\boldsymbol{\varrho}$ did not appear in Eq. (2) because, under the zero-range approximation, it integrates out with the corresponding part of the α-particle function to give an over-all normalization factor in the cross section. The zero-range approximation must be considered a possible fault in the approach; however, the error introduced by this approximation is not believed to be large.[13]

Equation (1) indicates that the individual-particle states γ contribute coherently to the theoretical cross section. The relative weights are determined by the structure factors G, where

$$G_{\gamma L1J} \equiv \beta_{\gamma L1J} \langle (l_1 \tfrac{1}{2})_{j1} (l_2 \tfrac{1}{2})_{j2} \mid (l_1 l_2)_L (\tfrac{1}{2} \tfrac{1}{2})_1 \rangle. \quad (5)$$

The coefficient $\beta_{\gamma L1J}$ measures the degree to which the ground state of $B+2$ has as its parent the residual nucleus B, plus two nucleons with the quantum numbers $\gamma (\equiv n_1 l_1 j_1 n_2 l_2 j_2)$, L, 1, and J. This parentage coefficient is analogous to the spectroscopic factors that appear in single-nucleon transfer theory.

We may define β more formally as

$$\beta_{\gamma L1J}(J_i, J_f) \equiv \binom{B+2}{2}^{1/2} \int [\Psi_{J_f}{}^{M_f}(\mathbf{B}) \Psi_{J\gamma}{}^{M}(\mathbf{r}_1, \mathbf{r}_2)]_J{}^{M_i} \times \Psi_{J_i}{}^{M_i}(\mathbf{B}; \mathbf{r}_1 \mathbf{r}_2)\, d\mathbf{B} d\mathbf{r}_1 d\mathbf{r}_2, \quad (6)$$

where the square bracket denotes vector coupling. The subscripts i and f refer to the target and residual nuclear states, respectively. The factor

$$\binom{B+2}{2}$$

is defined by

$$\binom{B+2}{2} = \frac{(N+1)!}{N!} \frac{(Z+1)!}{Z!} \quad \text{if isospin formalism is not used} \quad (7a)$$

and

$$\binom{B+2}{2} = \frac{(B+2)!}{B!} \quad \text{if isospin formalism is used.} \quad (7b)$$

It should be noted that N and Z (or B) refer only to the subgroup of nucleons from which the pair of nucleons is transferred in the pickup process.

It is apparent from Eq. (1) that for configuration mixing in the initial and final states, the configuration-mixture coefficients contribute coherently to the structure factors. That is, the two-nucleon transfer reactions are sensitive to the phases as well as the magnitudes of the mixture coefficients. The single-neutron transfer reaction, in contrast, depends only on the absolute value of these coefficients. It must be realized that it is, in general, impossible to deduce the magnitudes and relative phases of configurations contributing to two-nucleon transfer by analysis of the experimental data, since there are an infinite number of choices for the magnitudes and phases entering into G and $F_{L\gamma}$ which will generate similar cross sections.[14] On the other hand, if the wave functions obtained from a shell-model calculation are available, we can compute the structure factors and thus test in a very direct way whether the shell-model wave functions are indeed compatible with experimental results.

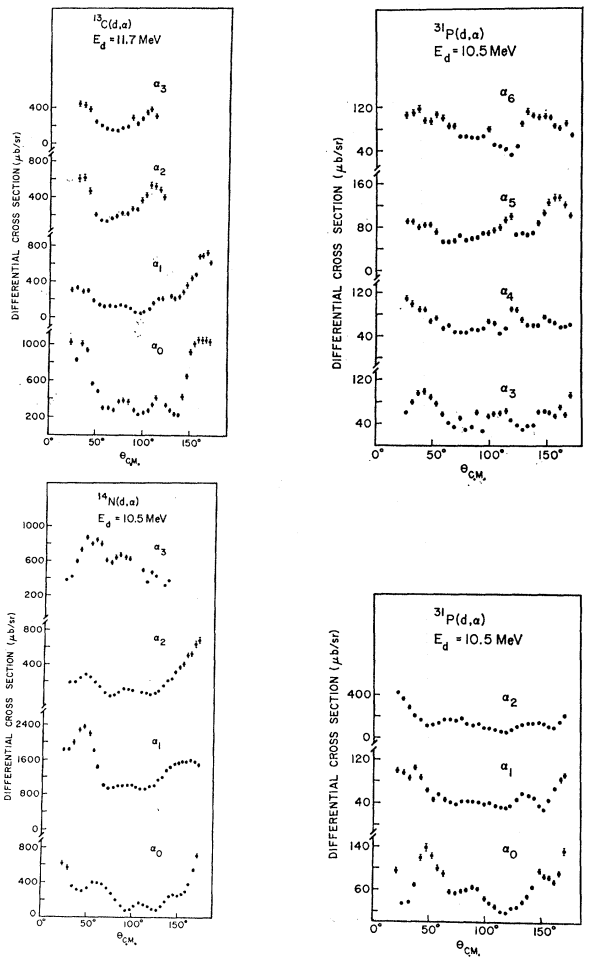

FIG. 4. Experimental angular distributions for the (d, α) reactions on ^{13}C, ^{14}N, and ^{31}P in the 10–12-MeV deuteron energy range.

[13] J. J. Wesolowski, L. F. Hansen, J. G. Vidal, and M. L. Stelts, Phys. Rev. **148**, 1063 (1966).

[14] N. K. Glendenning, Phys. Rev. **137**, B102 (1965).

TABLE I. Wave functions for the light nuclei.

Ref.	Nucleus	Level	J^π, T	Configurations in the $1p$ shell and above denoted by $(p_{3/2})^{n-x}(p_{1/2})^x$, where n = number of nucleons in $1p$ shell					
				$(p_{1/2})^2$	$(s_{1/2})^2$	$(d_{5/2})^2$	$(s_{1/2})(d_{3/2})$	$(d_{3/2})(d_{5/2})$	$(d_{3/2})^2$
19	^{14}N	0.00	$1^+, 0$	0.9666	0.0643	0.1839	0.1012	0.0105	−0.1318
				$(p_{1/2})^1$					
a	^{13}C	0.00	$\frac{1}{2}^-, \frac{1}{2}$	1.00					
				$(p_{1/2})^0$	$(p_{1/2})^1$	$(p_{1/2})^2$	$(p_{1/2})^3$	$(p_{1/2})^4$	
27	^{12}C	0.00	$0^+, 0$	0.487	0.000	0.402	0.072	0.039	
b	^{12}C	0.00	$0^+, 0$	0.375	0.000	0.458	0.065	0.102	
b	^{12}C	4.433	$2^+, 0$	0.000	0.465	0.162	0.313	0.060	
b	^{12}C	7.656	$0^+, 0$	0.180	0.000	0.730	0.010	0.070	
27	^{11}B	0.00	$\frac{3}{2}^-, \frac{1}{2}$	0.641	0.052	0.274	0.027	0.006	
b	^{11}B	0.00	$\frac{3}{2}^-, \frac{1}{2}$	0.463	0.060	0.404	0.045	0.028	
b	^{11}B	2.14	$\frac{1}{2}^-, \frac{1}{2}$	0.000	0.546	0.169	0.284	0.000	
b	^{11}B	4.46	$\frac{5}{2}^-, \frac{1}{2}$	0.000	0.533	0.125	0.327	0.015	
27	^{10}B	0.00	$3^+, 0$	0.654	0.225	0.108	0.011	0.001	
b	^{10}B	0.00	$3^+, 0$	0.574	0.185	0.210	0.017	0.013	

[a] W. W. True, Phys. Rev. **130**, 1530 (1963).

[b] I. Talmi and I. Unna, Ann. Rev. Nucl. Sci. **10**, 353 (1960).

IV. STRUCTURE INFORMATION

The numerical values of the nuclear structure factors β were calculated and fed into the form-factor program as parameters. The structure factors used in this work fall into two main categories—those for the light nuclei studies (^{14}N, ^{13}C, ^{12}C, ^{11}B, and ^{10}B) and those for the ^{31}P$(d, \alpha)^{29}$Si reactions. This division is necessary because the structure factors used for the ^{31}P work can be obtained in the isospin formalism, while those for the lighter nuclei studied must at present be computed by considering neutrons and protons separately. This is the case because the coefficients of fractional parentage (cfp's) which appear in the structure factors have been computed including isospin only for the case of three nucleons outside a closed core. The inclusion of isospin becomes extremely difficult if more than three nucleons are considered in the subgroup from which the pair is transferred. If a neutron is removed from a group of n_n neutrons in the j_n shell and a proton is removed from a group of n_p protons in the j_p shell such that the two nucleons are coupled to a total angular momentum J,

TABLE II. Structure factors for two-nucleon pickup from the light nuclei.

Set	Reaction	J	Structure factors for the various two-nucleon configurations[a]						
			$(p_{1/2})(p_{3/2})$	$(p_{3/2})^2$					
1	^{13}C(d, α_0)	1	0.7853	0.0901					
		2	1.0141	0.1163					
2	^{13}C(d, α_0)	1	0.5672	0.1039					
		2	0.7325	0.1342					
3	^{13}C(d, α_1)	1	0.0000	0.9457					
4	^{13}C(d, α_2)	3	0.0000	1.4102					
			$(p_{1/2})^2$	$(p_{3/2})^2$	$(s_{1/2})^2$	$(d_{5/2})^2$	$(s_{1/2})(d_{3/2})$	$(d_{3/2})(d_{5/2})$	$(d_{3/2})^2$
5	^{14}N(d, α_0)	1	0.4707	0.6731	0.0313	0.0896	0.0493	0.0051	−0.0642
6	^{14}N(d, α_0)	1	0.3625	0.7668	0.0241	0.0690	0.0379	0.0039	−0.0494
			$(p_{1/2})(p_{3/2})$	$(p_{3/2})^2$					
7	^{14}N(d, α_1)	1	0.5506	0.2712					
		2	0.7111	0.3501					
		3	0.0	0.4143					
			$(p_{1/2})^2$	$(p_{3/2})^2$					
8	^{14}N(d, α_2)	1	0.1740	−1.2222	0.0116	0.0331	0.0182	0.0019	−0.0237
9	^{12}C(d, α_0)	3	0.0	0.8094					

[a] The corresponding configurations are listed above each column of structure factors.

TABLE III. Structure factors for the $^{31}P(d, \alpha)$ reactions.

Set	Reaction	J	Structure factor	Two-nucleon configuration[a]
1	$^{31}P(d, \alpha_0)$	1	−0.8267	$(s_{1/2})^2$
			0.0035	$(s_{1/2})_p(d_{3/2})_n$
			0.0468	$(d_{3/2})^2$
2	$^{31}P(d, \alpha_1)$	1	0.0069	$(s_{1/2})^2$
			0.0086	$(d_{3/2})^2$
		2	0.2663	$(s_{1/2})_n(d_{3/2})_p$
			0.2414	$(s_{1/2})_p(d_{3/2})_n$
3	$^{31}P(d, \alpha_2)$	2	1.0675	$(s_{1/2})_p(d_{5/2})_n$
		3	1.2629	$(s_{1/2})_p(d_{5/2})_n$

[a] The subscripts p and n refer respectively to proton and neutron.

the nuclear-structure factor can be written as

$$\beta_{\gamma L1J}[(j_n^{n_n})J_a(j_p^{n_p})J_b; J_i \leftrightarrow (j_n^{n_n-1})J_1(j_p^{n_p-1})J_2; J_f] = (n_n n_p)^{1/2}(j_n^{n_n-1}J_1\}j_n^{n_n}J_a)(j_p^{n_p-1}J_2\}j_p^{n_p}J_b) \times \begin{bmatrix} J_1 & j_n & J_a \\ J_2 & j_p & J_b \\ J_f & J & J_i \end{bmatrix}. \quad (8)$$

Here, $(j^{n-1}J_1\}j^nJ_a)$ is a cfp necessary to expand a function of n particles in terms of a function of $n-1$ particles coupled to a single-particle function. The term in square brackets is the 9-j symbol times the square root factor $(\hat{J}_a\hat{J}_b\hat{J}_f\hat{J})^{1/2}$, such that $\hat{J} \equiv 2J+1$. When configuration mixing is present in the initial- and final-state wave functions, the structure factor becomes a sum of all the possible overlaps that can be obtained from Eq. (6). Each partial-structure factor is weighted by the appropriate product of the initial- and final-state configuration amplitudes. This is written explicitly as

$$\beta_{\gamma L1J}(J_i \leftrightarrow J_f) = \sum_{J_aJ_bJ_1J_2} C^{(1)}C^{(2)}\beta_{\gamma L1J}(J_aJ_b; J_i \leftrightarrow J_1J_2; J_f), \quad (9)$$

where $C^{(1)}$ and $C^{(2)}$ are the configuration amplitudes of the initial- and final-state wave functions, respectively, which would contribute to the appropriate two-particle configuration for the transferred pair.

The various wave functions employed for the initial- and final-state functions in the (d, α) reactions on ^{13}C, ^{14}N, and ^{12}C are listed in Table I. The source of each wave function is given in the Table. It should be noted that two sets of wave functions were available for many of the states. The amplitudes and relative phases for each configuration contributing to a given wave function are listed directly under the appropriate configuration notation.

In the present work, these various wave functions have been tested by extracting the spectroscopic information relevant to the two-nucleon transfer reactions studied and by comparing the results with the experimental cross sections of the various nuclear levels. The structure factors necessary for all the reactions studied in this nuclear-mass region are listed in Table II, along with the corresponding two-nucleon configurations in the wave function representing the transferred pair. The various structure factors, for each reaction, correspond to all allowed modes of two-particle pickup which connect the initial and final states. Again, two sets of structure factors are listed for some reactions where two sets of initial- and final-state wave functions were available. All of these structure factors are computed on the assumption that the two particles are simply picked up from the initial state to form the final-state wave function.

TABLE IV. Wave functions for ^{31}P and ^{29}Si.

Nucleus	Level	J^π, T	Amplitude	Configuration[a]
^{31}P	0.00	$\frac{1}{2}^+, \frac{1}{2}$	−0.6750	$s^3(J=\frac{1}{2}, T=\frac{1}{2})$
			0.0040	$s^2(J=1, T=0)d(J=\frac{3}{2}, T=\frac{1}{2})$
			−0.2880	$s(J=\frac{1}{2}, T=\frac{1}{2})d^2(J=0, T=1)$
			0.0270	$s(J=\frac{1}{2}, T=\frac{1}{2})d^2(J=1, T=0)$
			0.0070	$d^3(J=\frac{1}{2}, T=\frac{1}{2})$
^{29}Si	0.00	$\frac{1}{2}^+, \frac{1}{2}$	1.0000	$s(J=\frac{1}{2}, T=\frac{1}{2})$
^{29}Si	1.277	$\frac{3}{2}^+, \frac{1}{2}$	1.0000	$d(J=\frac{3}{2}, T=\frac{1}{2})$
^{29}Si	2.027	$\frac{5}{2}^+, \frac{1}{2}$	1.0000	$s^2(J=0, T=1)d^{-1}(J=\frac{5}{2}, T=\frac{1}{2})$

[a] The notation $s^2(J=1, T=0)d(J=\frac{3}{2}, T=\frac{1}{2})$ states that two nucleons in the $(2s_{1/2})$ shell couple to $J=1$ and $T=0$ and then this cluster is coupled to the third $(1d_{3/2})$ nucleon.

TABLE V. Bound-state parameters for cluster analyses. r(Coulomb) = 1.33 fm.

Reaction	L, J, N	Binding energy of cluster (MeV)	V_0 (MeV)	V_{s0} (MeV)	r_0 (fm)	a_0 (fm)
$^{13}C(d, \alpha_0)$	0, 1, 1	18.678	94.73	6.00	1.00	0.90
$^{13}C(d, \alpha_1)$	0, 1, 1	20.818	99.20	6.00	1.00	0.90
$^{14}N(d, \alpha_0)$	2, 1, 0	10.272	89.45	6.00	1.00	0.70
$^{31}P(d, \alpha_0)$	0, 1, 2	15.676	106.76	6.00	1.00	0.70

For the $^{31}P(d, \alpha_0)^{29}Si$ and $^{31}P(d, \alpha_1)^{29}Si$ reactions, the wave functions were taken from the shell-model calculations due to Glaudemans *et al.*[15] The ground state of ^{31}P was assumed to be composed of a ^{28}Si core plus three nucleons in the $1d_{3/2}$, $2s_{1/2}$ shell. The amplitudes and phases of the various possible configurations are shown in Table III. The ground and first excited states of ^{29}Si were taken to be pure single-particle levels, namely, a ^{28}Si core plus a $2s_{1/2}$ neutron for the ground state and a $1d_{3/2}$ neutron for the first excited state. A model of this type allows the inclusion of isospin formalism into the structure factors to give

$$\beta_{\gamma L1J}=\sqrt{3}\langle(j_2 j_3)[0, J]j_1; \tfrac{1}{2}\tfrac{1}{2}\}(j_1 j_2)[T'J']j_3; \tfrac{1}{2}\tfrac{1}{2}\rangle, \quad (10)$$

where the $\sqrt{3}$ factor represents the statistical factor for the three "active" particles outside the closed core. The angular-bracket term is the coefficient of fractional parentage necessary to expand explicitly the three-particle wave function in terms of two particles $(j_2 j_3)$ coupled to $T=0$, J, and then appropriately couple the "cluster" to the third nucleon (j_1) that is left after the transfer is accomplished. The isospin and angular momentum resulting from a two-particle coupling in the target wave function are respectively denoted by T' and J'. These two-particle couplings can be seen explicitly in several configurations of the wave functions listed in Table III. The cfp's in Eq. (10) are needed merely to couple the appropriate two particles transferred in the reaction and can be expressed in terms of 6-j symbols, as shown by Redlich.[16] We have omitted any discussion of the $LS \rightleftarrows jj$ coefficients, because they are well tabulated; the computer code which computes the form factors automatically includes the correct $LS \rightleftarrows jj$ coefficient in each term arising from the various two-particle configurations. The nuclear-structure factors are tabulated in Table IV, together with the corresponding two-particle configurations allowed in each case.

The wave function for the second excited state in ^{29}Si is based on the shell-model calculations of Wildenthal.[17] These calculations show that the dominant configuration (with an amplitude of about 0.6) of the second excited state of ^{29}Si consists of one hole in the $2d_{5/2}$ neutron shell, and two nucleons in the $2s_{1/2}$ shell. This dominant configuration was used in the $^{31}P(d, \alpha_2)^{29}Si$ structure-factor calculation; that is, the second excited state of ^{29}Si was represented by a hole in the $2d_{5/2}$ shell and two nucleons in the $2s_{1/2}$ shell. It was necessary to compute the $^{31}P(d, \alpha_2)^{29}Si$ structure factors by the methods used for the light nuclei, since, as was previously mentioned, the cfp's which include isospin have been explicitly written for cases involving only three particles. The $d_{5/2}$ hole would require cfp's involving 12 nucleons. The resulting structure factors are also shown in Table IV. It should be noted that all allowed J values are included in the tabulated structure factors. The corresponding L values allowed in each reaction will be discussed later.

V. ANALYSIS AND RESULTS

Two methods for computing the form factor were studied. The more exact method incorporated in Bayman's program has been described above. The second, and less accurate, method assumes that the transferred particles can be treated as a "cluster" or a unit, "heavy" nucleon of charge 1 and mass 2 bound in a Woods-Saxon potential, and having the quantum numbers of a deuteron with the appropriate angular momenta, L and J, allowed in the transfer reaction.

The appropriate bound-state wave functions corresponding to the cluster were computed by the code NEPTUNE, written by Tamura.[11] The cluster binding energy was set equal to the experimental separation energy for a deuteron from the target nucleus. The binding well depth was then adjusted by the program until an energy level with the proper quantum numbers $(NLJ, S=1)$ occurred at the experimental separation energy. The solution to the Schrödinger equation for this bound-state problem was then read into the DWBA part of the program. This DWBA code was identical to that used for the Bayman analysis, namely, code VENUS, also written by Tamura. All computations were carried out on the University of Texas CDC 6600 computer.

It should be pointed out that the various LJ contributions to the cross section were not summed in the cluster calculation as they were in the two-particle calculation. The incoherent sum was omitted, since the absolute normalization of a cluster calculation seems quite ambiguous. It is not very meaningful to worry

[15] P. W. M. Glaudemans, G. Wiechers, and P. J. Brussaard, Nucl. Phys. **56**, 548 (1964).
[16] M. G. Redlich, Phys. Rev. **99**, 1427 (1955).
[17] B. H. Wildenthal (private communication).

TABLE VI. Summary of all optical parameters.

Reaction	Set	Energy (MeV)	V (MeV)	W (MeV)	a_v (fm)	a_w (fm)	r_v (fm)	r_w (fm)	r_c (fm)	Ref.
$^{14}N(d, d)$	A	10.50	117.9	19.61	1.07	0.35	0.81	1.84	0.81	
$^{31}P(d, d)$	B	10.50	106.4	17.66	1.61	0.42	0.62	1.84	0.62	
$^{13}C(d, d)$	C	15.00	117.0	12.58	0.96	0.39	0.90	1.80	1.30	20
$^{12}C(d, d)$	D	34.40	92.41	9.75	0.79	0.69	1.04	1.43	1.30	22
$^{40}Ca(d, d)$	E	34.40	95.17	13.06	0.78	0.74	1.08	1.36	1.30	22
$^{12}C(\alpha, \alpha)$	a	18.00	200.0	4.00	0.50	0.30	1.97	1.87	1.30	
$^{12}C(\alpha, \alpha)$	b	14.00	100.0	4.00	0.60	0.60	1.77	1.77	1.30	21
$^{12}C(\alpha, \alpha)$	c	31.20	200.9	2.69	0.26	0.61	1.33	2.56	1.33	23
$^{28}Si(\alpha, \alpha)$	d	21.50	233.7	5.37	0.34	0.77	1.55	1.97	1.55	24
$^{26}Mg(\alpha, \alpha)$	e	44.00	209.2	35.79	0.50	0.37	1.48	1.50	1.48	25
$^{12}C(\alpha, \alpha)$	f	34.60	182.9	29.83	0.31	0.55	1.91	0.80	1.91	25

about how to weight each term in the sum over L and J, in such a case. Cluster calculations were made, however, for every possible LJ value in several of the reactions, and the best fits to the experimental data were compared with the dominant LJ contributions coming from the more exact analysis of Bayman. The various cluster parameters used in the computations of the bound-state wave functions for each reaction studied are shown in Table V.

The optical parameters used in the present analysis to generate the distorted waves in the incident and exit channels were obtained from the literature whenever possible. However, owing to the shortage of α-particle optical parameters, and the unavailability of deuteron parameters at the energies appropriate to the present work, it was necessary to perform an optical-model analysis on various elastic-scattering data to complete the list of necessary parameters.

The fits to the deuteron and α-particle elastic-scattering data were obtained with a computer code written by Smith.[18] In both types of analyses, fits were made using a potential with a surface-peaked imaginary well. The form of the optical potential used is

$$V(r) = -V_f(r, r_v, a_v) - i4a_wW(d/dr)f(r, r_w, a_w)$$

Central,

$$+(Ze^2/2r_d)(3-r^2/r_c^2) \quad \text{if } r \leq r_c \quad \text{Coulomb,} \quad (11)$$

$$+Ze^2/r \quad \text{if } r > r_c$$

where $f(r, r_v, a_v)$ [or $f(r, r_w, a_w)$] is the usual Woods-Saxon shape

$$f(r, r_v, a_v) = \{1+\exp[(r-r_v)A^{1/3}/a_v]\}^{-1}. \quad (12)$$

The optical parameters used in the present work are summarized in Table VI. Five sets of these parameters used were obtained from the literature as noted in the Table.[19–21] All remaining sets were determined from optical fits to elastic-scattering data. Only two sets of elastic scattering cross sections were measured in this work, namely, the $^{14}N(d, d)$ and $^{31}P(d, d)$ reactions at 10.5 MeV. The results of the deuteron optical-model analyses on these data and the corresponding optical parameters are shown in Fig. 5. The remaining data needed to complete the analyses were obtained from the literature.[22–24]

Although elastic-scattering analysis will usually produce several sets of parameters giving equally good fits, the present analysis revealed that the "$50\times A$" MeV well depths in both the entrance and exit channels invariably produced the best results in the DWBA calculations. These "deep" well depths correspond to values for the real optical potential of about 100 MeV for deuterons, and from about 150 to 200 MeV for the α particles. Although other parameters were tried, only values in this range produced reasonable results for the magnitudes and shapes of the various angular distributions. The absolute magnitudes of the (d, α) cross sections seemed to be particularly sensitive to the α-particle optical parameters.

In spite of the apparent limitations of the present theory, it was hoped that predictions of the absolute magnitudes of the cross sections would be possible, thus making detailed spectroscopic information attainable. It appears that the most ambiguous quantity entering the over-all normalization factors for the (d, α) cross section is the α-particle size parameter η. It was observed that only a 10% change in the size parameter produced a variation in the absolute magnitude of the cross section as large as 90%. Although various values for the α-particle size parameter were tried, the value of η used in this work was that given by Bayman,[12] namely, 0.260 fm^{-1}. This value was chosen because it gave reasonable normalization for the $^{31}P(d, \alpha_0)$ reaction at 33.7 MeV, where the mechanism should be predominantly direct and where good optical parameters were available from the literature. The absolute-value predictions for the reactions studied were tested by simply

[18] W. R. Smith, University of Southern California Report No. 136-119, 1967 (unpublished).
[19] L. J. Denes, W. W. Daehnick, and R. M. Drisko, Phys. Rev. **148**, 1098 (1966).
[20] E. B. Carter, G. E. Mitchell, and R. H. Davis, Phys. Rev. **133**, B1427 (1964).
[21] E. Newman, L. C. Becker, and B. M. Preedom, Nucl. Phys. **A100**, 225 (1967).
[22] T. Mikumo, J. Phys. Soc. Japan **16**, 1066 (1961).
[23] H. J. Fischbeck and W. M. Greenberg, Phys. Rev. **145**, 145 (1966).
[24] E. B. Carter (private communication).

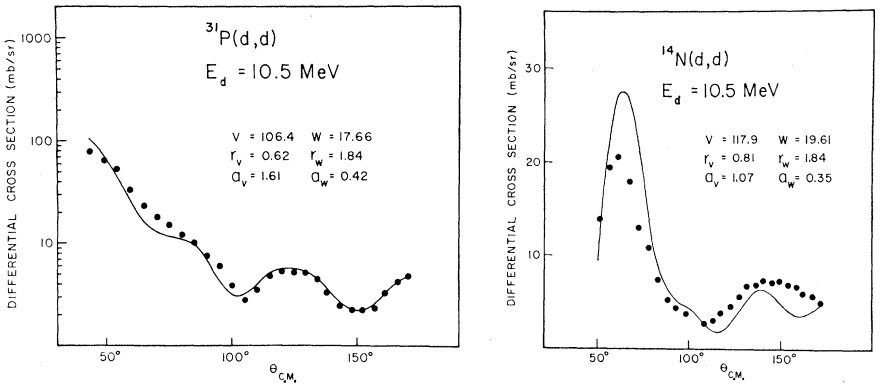

FIG. 5. Optical-model fits to the elastic ^{31}P(d, d) and ^{14}N(d, d) cross sections.

computing the ratio of experimental to theoretical cross section at the most forward peak in the angular distribution. These normalization factors are defined by

$$S \equiv \sigma_{\text{expt}}(\theta_1)/\sigma_{\text{theory}}(\theta_1),$$

where θ_1 is the angle at which the normalization is computed.

A. ^{31}P(d, α) Reaction

The theoretical fits to the experimental angular distributions for the α_0, α_1, and α_2 groups at the incident deuteron energy of 33.7 MeV are shown in Fig. 6. The deuteron and α optical parameters used are respectively denoted by E and e in Table VI. The angular momentum values allowed by the (d, α_0) reaction are L, $J=0$, 1 and 2, 1 while L, $J=0$, 1; 2, 1; and 2, 2 are allowed in the reaction leading to the first excited state of ^{29}Si. The ground-state reaction is characterized almost completely by an $L=0$, $J=1$ transfer. This multipole dominates the reaction by a factor of 6×10^3 over the $L=2$, $J=1$ contribution. The (d, α_1) reaction, on the other hand, is dominated by the $L=2, J=2$ contribution to the cross section, this term being about 10^4 times larger than the other two contributions. The L, J values allowed in the (d, α_2) reaction are L, $J=2$, 2 and 2, 3 with the $L=2$, $J=3$ contribution dominating by a factor of about 3.5. The shapes of the calculated angular distributions agree rather well with the experimental results. The normalization factor of 1.28 for the α_0 reaction represents a reasonable prediction of absolute magnitude for this cross section. The α_1 reaction, however, is underestimated by a factor of about 3 ($S=2.71$), and the α_2 reaction by a factor of about 2 ($S=1.82$). The experimental (d, α_2) cross section is, however, a factor of 10 greater than the (d, α_0) case. Thus, the *relative* magnitude of this (d, α_2) reaction is well predicted by the theory. To be more specific, if the normalization factor for the α_0 case is renormalized to unity, then the relative-magnitude predictions for the (d, α_1) and (d, α_2) reactions are respectively described by normalization factors of 2.1 and 1.4.

Absolute magnitude predictions for these reactions may be inaccurate in view of the apparent ambiguities in normalization of the theory; however, an explanation has been given for the wide range of relative intensities observed for levels in a given nucleus through two-nucleon transfer reactions.[14] The pair is transferred to or from the nucleus in a specifically correlated condition determined by the properties of the light nuclides. That is, the assumption of an $S=1$, $T=0$ state of the incident deuteron and an $S=0$, $T=0$ state of the outgoing α particle require the transferred pair to be coupled to $S=1$, $T=0$. The nuclear states will have greatly varying proportions of these appropriate correlations. The measure of the appropriate correlation and parentage as given in the structure factors of Table IV indicates a high degree of the necessary two-particle

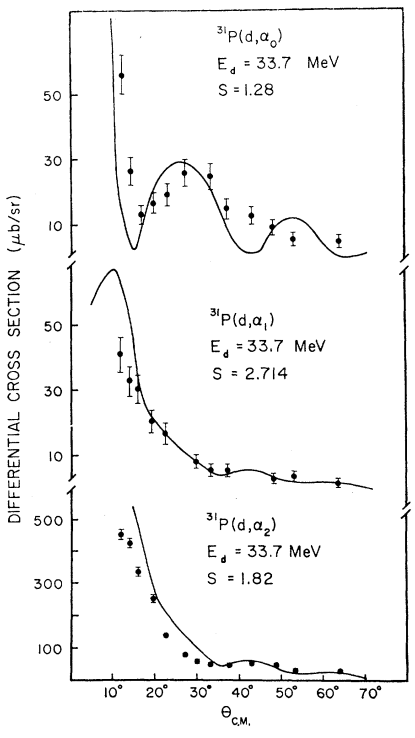

FIG. 6. Plots of experimental and theoretical angular distributions for the ^{31}P(d, α_{0-2}) reactions at 33.7 MeV.

correlation for the $^{31}P(d, \alpha_2)$ reaction; the structure factors are rather large compared to the $^{31}P(d, \alpha_0)$ and $^{31}P(d, \alpha_1)$ examples. This helps to explain the preferential population of the second excited state in ^{29}Si.

It is clear from this higher energy work on ^{31}P that, if optical parameters are well determined and the reaction dominantly direct, the two-nucleon theory is successful in fitting experimental angular distributions, and thus provides a powerful tool for examining the quality of theoretical nuclear wave functions.

A cluster calculation corresponding to the dominant $L=0$, $J=1$ term was computed for the $^{31}P(d, \alpha_0)$ reaction and the results are shown in Fig. 7. Unlike the lower energy results, to be shown later, this calculation displays a definite shift toward backward angles from the $L=0$, $J=1$ term of the more exact analysis. The quality of the shape fit, though, is still accurate enough to allow prediction of the dominant L, J value in the cross section.

The $^{31}P(d, \alpha)^{29}Si$ reaction study was repeated at a deuteron energy of 10.5 MeV to test the usefulness of the direct-reaction theory in this lower energy range. The reactions were believed to be predominantly direct even at 10.5 MeV, owing to the statistical analysis of Lock *et al.*[25] The incident- and exit-channel optical parameters are labeled, respectively, B and d in Table VI. The results of the DWBA calculations for the α_0 and α_1 reactions are shown in Fig. 8. Neither the shapes nor the absolute magnitudes are successfully predicted by the theory, with the backward angle fits being particularly bad. The poor quality of the fits, and the failure to observe the preferential excitation of the second excited state in ^{29}Si, suggest substantial compound-nucleus contribution to the cross sections at 10.5 MeV. It should be mentioned, however, that the α-particle optical parameters used in analyzing this

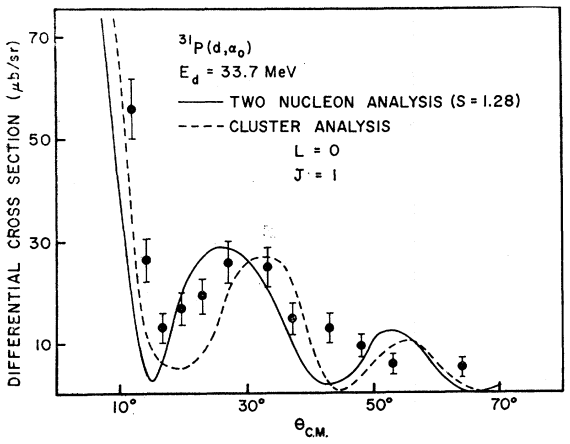

FIG. 7. Comparison of the cluster and two-particle DWBA calculations for $L=0$, $J=1$ in the $^{31}P(d, \alpha_0)$ reaction at 33.7 MeV.

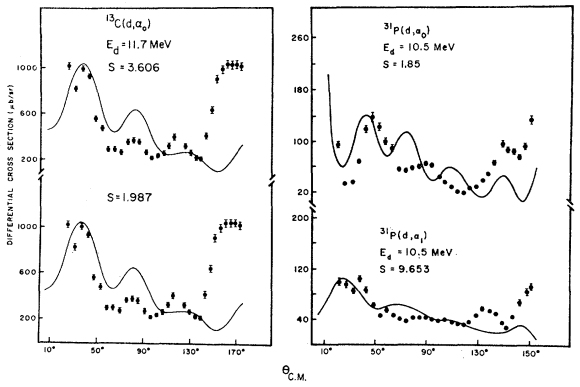

FIG. 8. Experimental and theoretical angular distributions for the $^{13}C(d, \alpha_0)$ reaction at 11.7 MeV and for the $^{31}P(d, \alpha_{0-1})$ reactions at 10.5 MeV. For the $^{13}C(d, \alpha_0)$ calculations, two separate wave functions have been used for the ground state of ^{11}B.

data gave a rather poor fit to the appropriate elastic-scattering data. Furthermore, the (d, α) calculations seem to be surprisingly sensitive to the α-particle parameters.

B. $^{13}C(d, \alpha)$ Reaction

The $^{13}C(d, \alpha)^{11}B$ cross sections were measured at a deuteron energy of 11.7 MeV; angular distributions leading to the ground and first excited state of ^{11}B were fitted. The incident- and exit-channel optical parameters used for the α_0 and α_1 reactions are those respectively denoted C and a in Table VI. The ^{13}C target nucleus was assumed to consist of a $1p_{1/2}$ neutron outside a closed core, as shown in Table I. Two sets of wave functions were available for the ground state of ^{11}B. One set was obtained from an earlier publication of Kurath[26] and the second set is due to more recent shell-model calculations by Kurath.[27]

Figure 8 shows the fits to the experimental angular distributions produced by these two wave functions for the ground state of ^{11}B. On the basis of absolute-magnitude prediction, the better results were those produced by the older Kurath wave functions, labeled (1) in Table I. This set produced the more pleasing normalization factor of 1.99. It should be noted that neither of the Kurath calculations determined the relative phases of the various configurations in the wave functions, which leads to some ambiguity since the two-nucleon transfer cross section is sensitive to the relative phases of the transfer configurations. The extracted two-nucleon wave function, however, involved only two configurations of the final state when computed on the basis of a pickup mechanism. Therefore, it was practical to try all possibilities for the relative phases associated with these terms $[a\,(p_{3/2})^2$ and $(p_{3/2})(p_{1/2})$ configuration$]$, there being only two phase possibilities. Essentially no difference was

[25] G. A. Lock, J. R. Curry, P. J. Riley, and C. G. Shugart, Phys. Rev. **176**, 1293 (1968).

[26] D. Kurath, Phys. Rev. **101**, 216 (1956).

[27] D. Kurath (private communication).

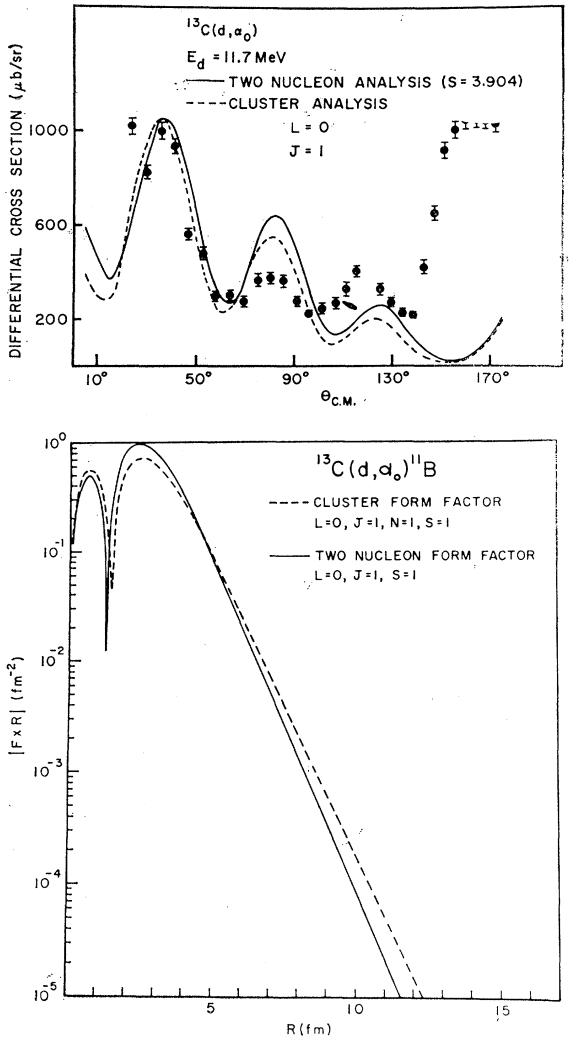

FIG. 9. Comparison of the cluster and two-particle calculations for $L=0$, $J=1$ in the $^{13}C(d, \alpha_0)$ reaction.

observed in the fit when the phases were changed from identical phases to opposite phases.

The allowed angular-momentum values in this transfer are $L, J=0, 1; 2, 1;$ and 2, 2. The contributions from $L, J=0$, 1 and 2, 2 dominate the reaction, both being about 12 times larger than the $L=2, J=1$ term. A cluster-model calculation was also applied to this $^{13}C(d, \alpha_0)$ data. The only L, J value in this analysis giving a reasonable fit to the data was the $L=0, J=1$ case. This fit was arbitrarily normalized to the data and is compared with the dominant $L=0, J=1$ contribution from the more exact analysis in Fig. 9. The agreement between the two calculations is excellent. It would therefore be anticipated that the cluster form factor very closely approximates the $L=0, J=1$ form factor in the Bayman analysis. Indeed, this is also seen to be true in Fig. 9.

The lack of agreement between theory and experiment at the backward angles and the relative symmetry about 90° for this experimental data are indications that a compound-nucleus mechanism might give an important contribution to this reaction also.

The analysis of the $^{13}C(d, \alpha_1)$ reaction is given in Fig. 10. The shape of the theoretical angular distribution is in fair agreement with experiment and the normalization factor of 0.94 indicates an excellent prediction of absolute magnitude. The allowed angular momenta for this reaction were $L, J=0$, 1 and 2, 1; the contribution from $L=0$, $J=1$ dominated the reaction by a factor of about 12. This dominant term is compared with the corresponding cluster analysis and is also shown in Fig. 10. Again, these two calculations are almost indistinguishable.

C. $^{14}N(d, \alpha)$ Reaction

These reactions have previously been investigated by Pehl at 15 MeV.[28] The optical parameters describing the incident and exit channels for both the α_0 and α_1 reactions are labeled respectively A and c in Table VI. The α-particle parameters which are denoted a were used in the analysis of the (d, α_2) reaction. Again, two sets of wave functions for the residual nucleus, ^{12}C, were also available from the Kurath calculations for the

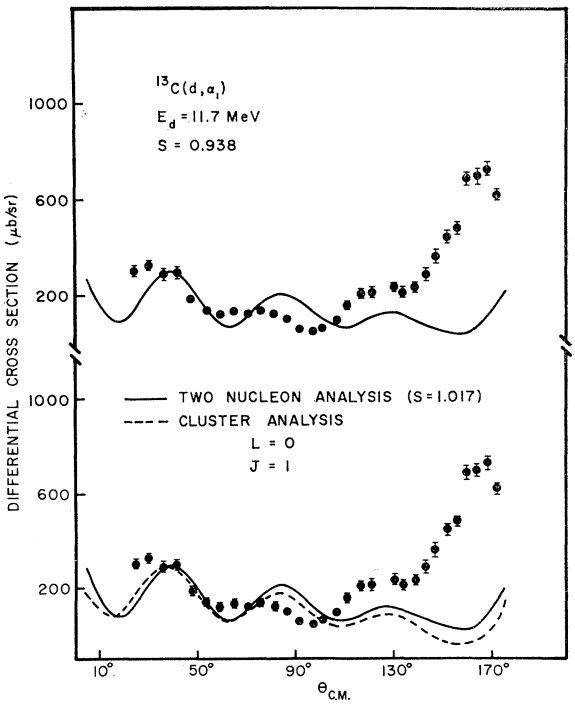

FIG. 10. Plots of experimental and theoretical angular distributions for the $^{13}C(d, \alpha_1)$ reaction. The bottom curve shows a comparison of the cluster and two-particle calculations for $L=0$, $J=1$.

[28] R. H. Pehl, Ph.D. dissertation, University of California Report No. UCRL-10993, 1963 (unpublished).

ground-state reaction, although the relative phases for the various configurations were not known. However, as in the ^{13}C work, only two configurations of the final-state wave function were involved in the two-particle transfer function. In contrast to the ^{13}C work, changing the relative phases of these two terms in the ^{12}C wave function produced a definite change in the absolute magnitude of the cross section; it was increased by a factor of 6 when opposite phases were used. The more reasonable result of 1.22 for the normalization factor S was obtained when the phases were identical in the older Kurath wave functions. A comparison with the more recent shell-model calculations of Kurath is shown in Fig. 11. It is interesting to note that in this ^{14}N(d, α_0) case, the newer Kurath functions do not even predict the shape of the angular distribution. The fit produced by the set of structure factors labeled (5) in Table II is reasonably good and the ratio of experimental to theoretical magnitude is almost unity. Only a slight angular shift is apparent between the theoretical and experimental angular distributions.

The allowed L, J values in this reaction were 0, 1 and 2, 1, with the $L=2$, $J=1$ case dominating by a factor of 6. A cluster calculation corresponding to this dominant contribution was also performed and the results are shown in Fig. 12. As before, the cluster calculation is almost identical to the dominant $L=2$, $J=1$ "exact" calculation. The form factors calculated using these two methods are compared in Fig. 12. Although the shapes of the two form factors are very similar, their magnitudes differ by as much as a factor of 3. This is believed to be due to the rather complex two-nucleon configuration for the ^{14}N(d, α_0) reaction. It is somewhat surprising that both the two DWBA cross sections and the two form factors agree so well in shape, in view of the large difference in the details of computing the two form factors. This comparison, along with the previous results, seems to indicate that the cluster calculation is always sufficient to determine dominant L, J values in a direct reaction. Also, the difference between the single

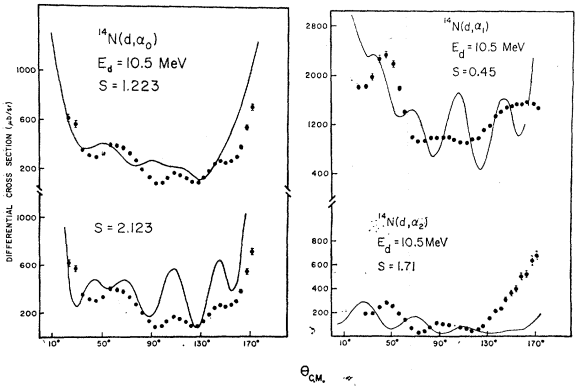

FIG. 11. Plots of experimental and theoretical angular distributions for the ^{14}N(d, α_{0-2}) reactions. In the ^{14}N(d, α_0) calculations, two different wave functions have been employed for the ground state of ^{12}C.

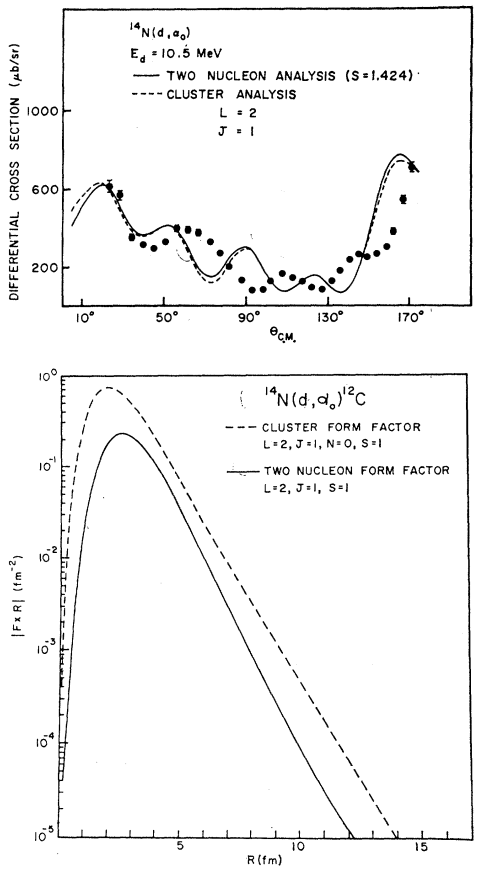

FIG. 12. Comparison of the cluster and two-particle calculations for $L=2$, $J=1$ in the ^{14}N(d, α_0) reaction.

dominant term fit and the fit including both possible L, J values indicate that the relative contributions from each multipole must be correctly taken into account to achieve the most meaningful results. This can only be accomplished by using a single-particle basis to construct the two-nucleon form factor. Further, a normalization problem in the cluster calculation is indicated by the deviation in the magnitude of the form factor relative to that of the exact calculation. This would preclude accurate normalization for a given multipole in the cluster calculation.

The analyses of the ^{14}N(d, α_1) and ^{14}N(d, α_2) reactions are also shown in Fig. 11. Neither of these experimental sets of data is well fit by the two-nucleon-DWBA theory. The major source of uncertainty in the analysis of these data seems to be in the α-particle optical parameters. α-particle elastic scattering reveals many resonances in the energy region appropriate to these experiments.[24]

VI. SUMMARY

From the results presented, the extraction of spectroscopic information from direct two-nucleon transfer reactions seems to be within the scope of the present

theoretical framework. The computed cross sections were sufficiently sensitive to the phases and amplitudes of the two-nucleon wave functions to allow a definitive test of nuclear wave functions involved in the (d, α) reactions, as was clearly demonstrated for the $^{14}N(d, \alpha_0)$ reaction. Although the $^{13}C(d, \alpha_0)$ calculation showed little dependence on a variation of the phases, the $^{14}N(d, \alpha_0)^{12}C$ analysis definitely required the two contributing terms in the ^{12}C wave function to have identical phases. This sensitivity, on the other hand, can be destroyed by poor optical parameters and strong contributions from compound-nuclear mechanisms. Indeed, the theoretical cross sections seem to be very sensitive to the α-particle optical parameters.

As anticipated, the most favorable and most reliable results were those obtained from the $^{31}P(d, \alpha)$ work at 33.7 MeV. It is encouraging to note, however, that all of the (d, α_0) reactions studied were reasonably well fit by the theory and the absolute-magnitude predictions were consistently found to be within a factor of 2 from the experimental values. This is certainly comparable to the successes of other work presented in the literature. In fact, the *relative* magnitudes predicted by the present theory are in quite good agreement with the experimental results. If the theory is normalized to the $^{31}P(d, \alpha_0)$ case at 33.7 MeV, then the *maximum* deviation from unity for all the (d, α_0) relative normalization factors is found to be represented by the value of 1.56 for the $^{13}C(d, \alpha_0)$ analysis.

The results of the cluster analyses definitely indicate that such an approximation to two-nucleon transfer theory is capable of predicting the dominant angular-momentum transfer contributing to a particular cross section. In fact, the only significant difference between the form factors computed by the cluster approximation and the exact method seems to be in their absolute magnitudes. Although this precludes any determination of relative multipole strengths, the determination of L values falls well within the limitations of such a calculation.

The real test, however, of a direct-reaction theory lies in its ability to predict relative magnitudes for various reactions. The present theory is seen to be capable of meeting this requirement with a fair degree of success if good optical parameters are available, and if the reaction proceeds dominantly through a direct mechanism. On the other hand, it is not surprising that the most ambiguous part of the theory, namely, the prediction of absolute cross sections, becomes less exact for states other than the ground state in a (d, α) reaction. The complete description of absolute magnitudes would, thus, be highly desirable for a detailed spectroscopic analysis with two-nucleon pickup reactions. Additional work on the absolute normalization of such two-particle transfer cross sections should lend added strength to the spectroscopic capabilities of such a theory. Further, the need for more α-particle elastic-scattering data and optical-model analyses is obvious.

The success of the present study should encourage additional refinements to the theory to include finite-range effects and the influence of nonlocality of the optical potentials. These refinements, along with additional work on absolute normalization problems, will probably lead to a reliable method of gathering detailed nuclear-structure information through direct two-nucleon transfer reactions.

ACKNOWLEDGMENTS

We wish to thank Dr. B. F. Bayman for valuable discussions and for providing a computer code necessary for the calculations. Helpful discussions with Dr. T. A. Griffy are also acknowledged. Thanks are due to Dr. E. Newman and Dr. B. H. Wildenthal for their assistance in obtaining the data taken with the Oak Ridge Isochronous Cyclotron. The hospitality of the staff of the Electronuclear Division of the Oak Ridge National Laboratory is gratefully acknowledged. Research participation at Oak Ridge National Laboratory for two of us (J. R. Curry and P. J. Riley) was sponsored by Oak Ridge Associated Universities. We also thank Dr. G. A. Lock, Dr. P. A. Moore, and Dr. C. G. Shugart for their assistance in taking the lower-energy data. One of us (J. R. Curry) acknowledges financial support from an Atomic Energy Commission Special Fellowship in Nuclear Science and Engineering. Finally, we wish to thank B. M. Foreman for writing the manuscript.